ORIGINAL ARTICLE – CANCER RESEARCH

CrossMark

Patient-derived, three-dimensional spheroid cultures provide a versatile translational model for the study of organ-confined prostate cancer

Johannes Linxweiler[1] · Markus Hammer[1] · Stefanie Muhs[1] · Moritz Kohn[1] · Alexej Pryalukhin[2] · Christian Veith[2] · Rainer M. Bohle[2] · Michael Stöckle[1] · Kerstin Junker[1] · Matthias Saar[1]

Abstract

Purpose To generate and characterize 3D spheroid suspension cultures from radical prostatectomy (RP) specimens as a versatile model system for organ-confined prostate cancer (PCa).

Methods Cancerous tissue samples from RP specimens were excised by a uropathologist. Preparation of 3D spheroids was done by mechanical disintegration and limited enzymatic digestion followed by serial filtration through 100 µm- and 40 µm-cell strainers. Thereafter, spheroids were cultured in a modified stem cell medium and characterized by a live/dead assay, whole-spheroid immunohistochemistry (IHC; CK5, CK8, AMACR, PSA, Ki67, AR, αSMA, Vimentin, E-Cadherin) and PSA-measurements in culture medium. Furthermore, their response to pharmaceutical treatment with docetaxel, bicalutamide, enzalutamide and abiraterone was tested.

Results 173 RP cases were included. The median preoperative PSA-level was 16.12 ng/ml [range 0.99;345], the median Gleason score was 7b [6;10]. 64 cases were excluded due to low tumor content in frozen sections (43) or to insufficient spheroid formation (21). In the remaining 109 cases, spheroids formed successfully and stayed viable for up to several months. IHC analysis revealed AR-, CK8-, and AMACR-positivity in nearly all cases, while CK5-positive cells were detectable only occasionally as were α-SMA and Vimentin. E-Cadherin was positive in most cases. Furthermore, spheroids proved to be amenable to cryopreservation. While abiraterone had no effect and docetaxel only a moderate effect, spheroid viability was markedly reduced upon bicalutamide and enzalutamide treatment.

Conclusions Multicellular 3D spheroids can be generated from patient-derived RP tissue samples and serve as an innovative in vitro model of organ-confined PCa.

Keywords 3D · In vitro model · Organ-confined · Organoid · Prostate cancer · Spheroid culture

✉ Matthias Saar
matthias.saar@uks.eu

1 Department of Urology, Saarland University, Homburg, Saar, Germany

2 Department of General and Surgical Pathology, Saarland University, Homburg, Saar, Germany

Introduction

In men, prostate cancer (PCa) is the most commonly diagnosed cancer and the second leading cause of cancer-related deaths in the USA and Europe (Siegel et al. 2016; Wong et al. 2016). Despite recent advances in the fields of early detection (Koppers-Lalic et al. 2016), diagnostics (Ahmed et al. 2017) and therapy (Fizazi et al. 2017; Shipley et al. 2017) as well as in the understanding of the molecular mechanisms underlying disease development and progression (Fraser et al. 2017; Ku et al. 2017), there are still many important questions that remain unresolved in this molecularly and clinically extremely heterogeneous disease. Further improvements in patient care are mainly hampered by a lack of representative preclinical models to study organ-confined

PCa in vitro. There are numerous well-characterized PCa cell lines available, yet they were all established from metastases (Wu et al. 2013). This contrasts to the fact, that the majority of patients newly diagnosed with PCa present with organ-confined disease in times of widely adopted PSA-screening (Shao et al. 2009). However, primary cell cultures from prostatectomy material proved to be extremely difficult to raise and maintain (Peehl 2005; Chen et al. 2012). In recent years, three-dimensional organoid cultures derived from patient tissue samples have emerged as a promising new approach to overcome constraints inherent with the use of conventional monolayer-cultures in various types of cancer including PCa (van de Wetering et al. 2015; Boj et al. 2015; Wang et al. 2017). Besides, a fair representation of intra- and intertumor-heterogeneity (as opposed to the monoclonal nature of established cell lines), other strengths of this model system include a better modeling of the organ-specific tumor microenvironment as well as the three-dimensional tissue architecture with appropriate oxygen, nutrient and drug concentration gradients. Of note, the group of Hans Clevers recently reported on the generation and in-depth molecular characterization of three-dimensional organoid cultures from patients with advanced prostate cancer (Gao et al. 2014; Drost et al. 2016). They used biopsy specimens (metastases) as well as circulating tumor cells (CTCs) to establish seven long-term organoid cultures, which recapitulated well the molecular diversity of PCa subtypes including *TMPRSS2-ERG* fusion, *SPOP* mutation, *SPINK1* overexpression and *CHD1* loss (Barbieri et al. 2012; Cancer Genome Atlas Research Network 2015). However, to date there is only one report with very limited data on the generation of three-dimensional spheroid cultures from radical prostatectomy (RP) tissue samples representing organ-confined PCa (Caspar et al. 2016).

In this study, we aimed to generate and characterize three-dimensional spheroid cultures from a large number of radical prostatectomy specimens and to test their amenability to cryopreservation and in vitro drug testing.

Materials and methods

Patient selection and tissue acquisition

There were no strict inclusion or exclusion criteria for the selection of RP cases since we aimed to cover the whole spectrum from low-volume Gleason 6 to locally advanced high-risk disease in our cohort. However, cases with multiple positive biopsy cores on one side of the gland as well as cases with palpable tumors were preferred due to a higher probability of successful retrieval of cancerous tissue.

Immediately after removal, the whole prostatectomy specimen was put in a cooled sterile container and transferred to the pathology department. After careful visual and palpatory examination (also taking into account preoperative data like biopsy results or prostate-MRI), a presumably cancer-bearing tissue sample was excised from the RP specimen by one of three experienced uropathologists (AP, CV, RMB) and put into cell culture medium until the initiation of the actual spheroid generation procedure. To ensure sufficient tumor cell content in the retrieved samples ($> 50\%$ tumor cells), a fresh-frozen section was prepared from each sample, H&E-stained and microscopically examined.

Generation and cultivation of spheroids

For the generation of three-dimensional spheroids, the tissue sample obtained from the RP specimen was first put in a sterile petri dish and covered with lysis solution. The latter was composed of DMEM cell culture medium (Sigma-Aldrich, St. Louis, USA) supplemented with 1% penicillin/streptomycin (Sigma-Aldrich, St. Louis, USA) and collagenase IA (100 Units/ml; Sigma-Aldrich, St. Louis, USA) or Liberase TM collagenase I/II mix (0.25 Wünsch Units/ml; Roche, Basel, Switzerland) according to the manufacturer´s instructions. Then, the tissue sample was dissected into about 0.5 mm small pieces using two scalpels. Afterwards, the dissected tissue was incubated in the lysis solution at 37 °C and 10% CO_2. This process of limited enzymatic digestion was performed under repetitive visual control and under repetitive mixing by pipetting and/or vortexing until well-defined spheroids had formed. Then, the cell suspension was washed in PBS (Thermo Fisher, Waltham, USA) and filtered through 100 µm and 40 µm cell strainers (Greiner, Kremsmünster, Austria). Subsequently, the different cell fractions (> 100 µm, 100-40 µm, single cells) were cultivated in ultra-low attachment multiwell plates (6-, 24- or 96-well format; Corning Inc., Corning, USA) in a modified stem cell medium (further referred to as "StemPro medium"). This StemPro medium was composed of (for a total volume of 100 ml) 89.8 ml Gibco GlutaMAX DMEM/F-12 (Thermo Fisher, Waltham, USA), 7.2 ml 25% BSA (Thermo Fisher, Waltham, USA), 182 µl 2-Mercaptoethanol (Thermo Fisher, Waltham, USA), 2 ml StemPro® hESC Supplement (Thermo Fisher, Waltham, USA), 1 ml penicillin/streptomycin (Sigma-Aldrich, St. Louis, USA), 50 µl 200 nM R1881 (Sigma-Aldrich, St. Louis, USA), 8 µl FGF-b (100 µg/ml; Thermo Fisher, Waltham, USA) and 20 µl Y-27632 dihydrochloride (14 mg/ml; Sigma-Aldrich, St. Louis, USA). In single cases, PrEGM™ medium was used, which was obtained from Lonza (Base, Switzerland) and prepared according to the manufacturer's instructions. Noggin and Spondin were purchased from Peprotech (Hamburg, Germany) and used in a final concentration of 100 ng/ml (Noggin) and 500 ng/ml (Spondin), respectively. Culture medium was changed at least every third day. If cells

reaggregated to very large clusters or the initial digestion proved to be insufficient, enzymatic digestion was repeated after initial cultivation using Liberase TM or Trypsin/EDTA (Thermo Fisher, Waltham, USA). To count cells, the spheroids were digested to single cells with Trypsin/EDTA and subsequently counted using a Neubauer chamber. During cultivation, viability of the spheroids was regularly monitored by a live/dead assay.

Histology and immunohistochemistry (IHC)

For histological examination, spheroids were embedded in a cylinder of agarose gel (Sigma-Aldrich, St. Louis, USA) in the lower part of a 1.5 ml Eppendorf tube (Eppendorf, Hamburg, Germany). Thereafter, the agarose cylinder containing the spheroids was fixed in formalin and embedded in paraffin using standard protocols. H&E staining and immunohistochemistry (IHC) were performed as previously described (Linxweiler et al. 2012) using antibodies against alpha-methyl-CoA-racemase (AMACR; 1:100; Diagnostic BioSystems, Pleasanton, USA), androgen receptor (AR; 1:200; Sigma-Aldrich, St. Louis, USA), alpha smooth muscle actin (αSMA; 1:200; Dako, Glostrup, Denmark), CD56 (1:200; Abcam, Cambridge, UK), Chromogranin A (1:100; Dako, Glostrup, Denmark), cytokeratin 5 (CK5; 1:50; Diagnostic BioSystems, Pleasanton, USA), cytokeratin 8 (CK8; 1:200; Sigma-Aldrich, St. Louis, USA), Ki67 (1:50;), prostate-specific antigen (PSA; 1:50; Dako, Glostrup, Denmark), Synaptophysin (1:400; Sigma-Aldrich, St. Louis, USA) and Vimentin (1:100; Dako, Glostrup, Denmark).

Cell culture assays, pharmaceutical treatment, PSA measurement

Live/dead viability/cytotoxicity assays (Life Technologies, Carlsbad, USA) and MTS cell proliferation assays (Promega, Madison, USA) were used according to the manufacturers' instructions. Pharmaceutical treatment of the spheroid cultures was performed with Abiraterone Acetate (20 µM; SelleckChem, Houston, USA), Bicalutamide (100 µM; SelleckChem, Houston, USA), Enzalutamide (200 µM; SelleckChem, Houston, USA) and Docetaxel (5 nM; SelleckChem, Houston, USA). First, spheroids were seeded in 96-well plates in triplicates in a concentration of 5×10^3 or 1×10^4 cells. Whenever possible—according to the number of available cells—experiments were performed with both cell counts. However, if starting material was limited, just one approach with 1×10^4 cells per well was performed. After 1 day (day 1), the viability of the untreated cells was analyzed using a MTS assay and the acquired signal was set to 100%. Thereafter, pharmaceutical treatment with the above-mentioned compounds was started and the viability of untreated and treated cells was again analyzed two (day 3) or four (day 5) days later. In general, the 100–40 µm spheroid fraction was used for cell culture assays. PSA measurement in cell culture medium was performed using an Electo-ChemiLuminescence ImmunoAssay (ECLIA) in a COBAS® immunoassay system (Roche, Basel, Switzerland) according to the manufacturer's instructions.

Results

Generation and cultivation of spheroids

We included 173 RP cases with a median age of 67 years (range 48;82), a median preoperative PSA of 16.12 ng/ml (range 0.99;345) and a median Gleason score of $4 + 3 = 7b$ (range 6;10). The median weight of tissue provided by the pathologists for further processing was 214.2 mg (range 23.1;2386). 64 cases (37%) were excluded due to low tumor content in fresh-frozen sections (43 cases; 25%) and insufficient spheroid formation (21 cases; 12%). From the remaining 109 cases, spheroids could be successfully generated and these could be cultivated for a median time of 19 days (range 4;100) (Fig. 1). While spheroids in the > 100 µm fraction often showed central necrosis, this was not observed in the 40–100 µm fraction. A significant association between Gleason score and the success rate of spheroid formation or the time spheroids stayed viable in culture was not observed. However, cancer cells from Gleason 6 or 7 tumors tended to more efficiently form spheroids compared to Gleason 8, 9 or 10 tumors.

### Optimizing of enzymatic digestion and culture conditions

After mechanical workup, two different enzymes/enzyme mixes—collagenase IA and Liberase TM (a collagenase I/II mix)—were tested for limited enzymatic digestion using tissue specimens from the same case ($n = 5$). Liberase TM consistently showed better tissue disintegration with separation of a larger number of homogenous spheroids. Additionally, the spheroids generated by Liberase TM digestion were more vital than those generated by collagenase IA digestion (Fig. 2a). We further examined the influence of different concentrations of the synthetic androgen R1881 in the culture medium on spheroid formation and long-term viability (Table 1). Here, a tendency towards a slightly longer survival of the spheroids with 0.1 nM R1881 was seen, however the differences observed were not significant. Accordingly, a R1881 concentration of 0.1 nM was used henceforward. Besides that, another cell culture medium specially designed for the cultivation of primary prostate epithelial cells (PrEGM™) was tested.
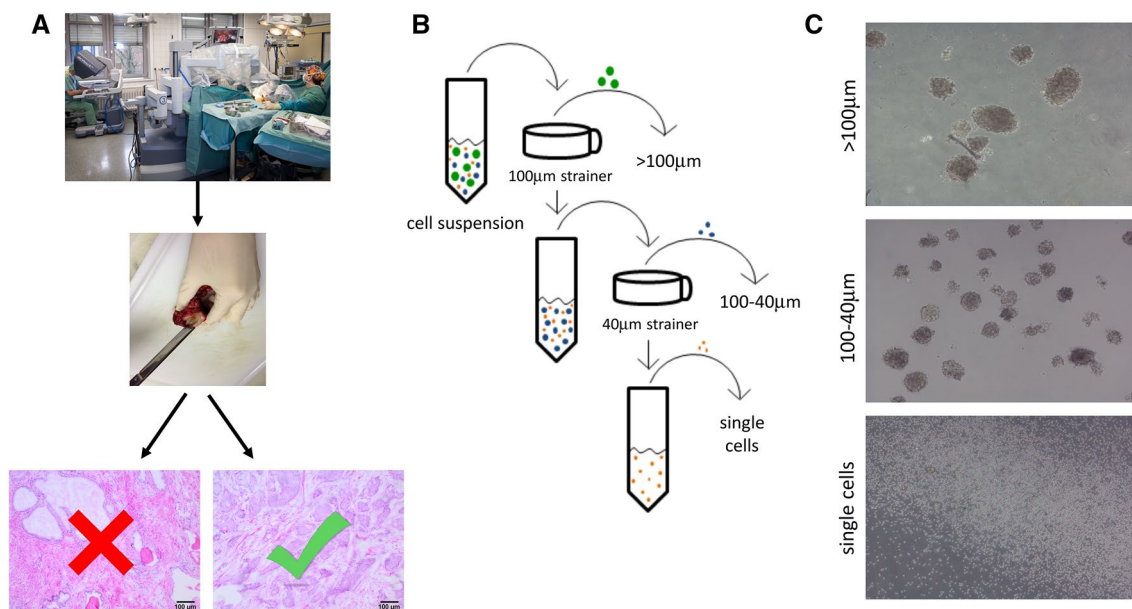
Fig. 1 Generation and cultivation of spheroids from RP tissue specimens. **a** After radical prostatectomy (RP), the whole specimen is put on ice and transferred to a uropathologist that dissects a small, presumably cancerous tissue piece. Sufficient tumor cell content is proven by H&E-stained fresh-frozen section. **b** After mechanical workup and limited enzymatic digestion, the cell suspension is filtered through 100 μm and 40 μm cell strainers yielding **c** three cell fractions (spheroids > 100 μm, spheroids 100–40 μm, single cells) which are cultivated separately

Fig. 2 Optimizing of enzymatic digestion and applicability to cryopreservation. **a** Microphotographs of cultivated tissue/spheroids 1 (upper row) and 3 (middle row) days after enzymatic digestions with collagenase IA (left column) or Liberase TM (right column). Live/dead assay (lower row) 3 days after enzymatic digestion with collagenase I (left) or Liberase TM (right). Green fluorescent signals indicate viable, red fluorescent signals indicate dead cells. **b** Live/dead assay before (upper image) and after (lower image) 1 week of cryopreservation in liquid nitrogen
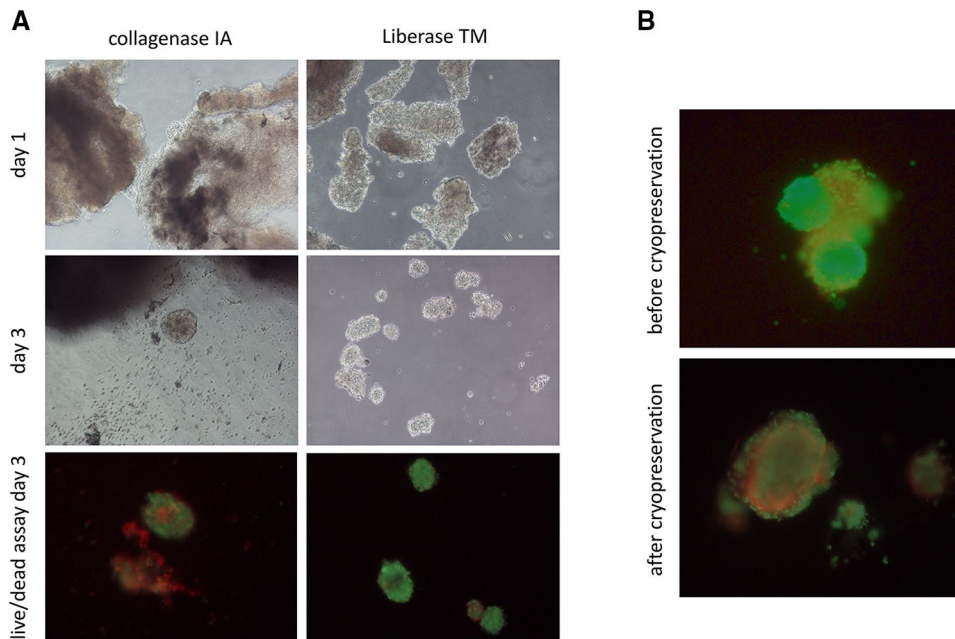
However, no differences in spheroid viability after 8 days of culture could be seen compared to the established StemPro medium (supplementary Fig. 1). The addition of Noggin and Spondin to StemPro medium did also not result in more efficient spheroid formation or better spheroid viability (data not shown).

Cryopreservation

To test the amenability of primary spheroids to cryopreservation, spheroids were stored in liquid nitrogen in a cryopreservation solution (stem cell medium containing 10% DMSO) for 1 week ($n = 3$). A live/dead assay was performed 1 day before freezing and 1 day after thawing and showed

Table 1 Effect of R1881-concentration in culture medium on spheroid viability

R1881 concentration (nM)	10	1	0.1	0.01
$n=$	6	16	37	19
Viability in culture in days; median (range)	19 (4;34)	16.5 (6;100)	20.5 (4;81)	18 (4;63)

Table 3 Immunohistochemical characterization

	Positive	Negative
AMACR	21 (91%)	2 (9%)
AR	16 (94%)	1 (6%)
PSA	7 (29%)	17 (71%)
CK5	18 (75%)	6 (25%)
CK8	21 (88%)	3 (12%)
Ki67	8 (33%)	16 (67%)
Vimentin	11 (79%)	3 (21%)
α-SMA	9 (64%)	5 (36%)

AMACR alpha-methyl-CoA-racemase, *AR* androgen receptor, *PSA* prostate-specific antigen, *CK5* cytokeratin 5, *CK8* cytokeratin 8, *α-SMA* alpha smooth muscle actin

that the spheroids were still alive after thawing, yet their viability was slightly reduced (Fig. 2b).

Immunohistochemistry

Whole-spheroid immunohistochemical stainings showed positive reactions for the luminal marker CK8 in the majority of cases. Of note, single cells staining positive for the basal marker CK5 were also detected in 75% of cases (Fig. 3a). *AMACR* overexpression was present in almost all cases as was strong cytoplasmic expression of *AR* (Fig. 3b). Ki67-positive cells were only rarely detected. PSA expression was fairly heterogeneous, however, elevated PSA-levels in the cell culture medium of the spheroids could also be consistently detected when PSA immunohistochemistry was negative (Table 2). The mesenchymal markers Vimentin and α-SMA stained positive in single dispersed cells in 71% and

79% of cases, respectively, suggesting the presence of (activated) fibroblasts in the spheroids. The detailed results of immunohistochemical stainings are summarized in Table 3. Note, that the number of patient-derived spheroids stained for a single antibody varies due to the limited number of representative FFPE sections that could be generated from each case.

To test for a neuroendocrine transdifferentiation of the cultivated PCa cells under in vitro conditions, we stained the
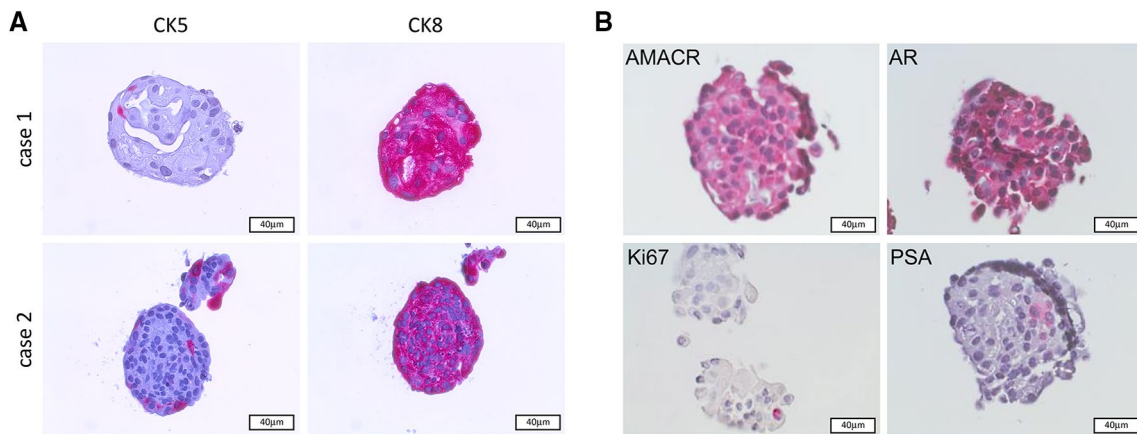
Fig. 3 Immunohistochemistry. **a** CK5- and CK8-staining from two representative cases. **b** Representative microphotographs of spheroids stained for AMACR, AR, Ki67, and PSA. ×400 magnification. *AMACR* alpha-methyl-CoA-racemase, *AR* androgen receptor, *PSA* prostate-specific antigen, *CK5* cytokeratin 5, *CK8* cytokeratin 8

Table 2 Measurement of PSA-levels in culture medium

Case	1	2	3	4	5	6	7	8	9
PSA IHC	−	+	−	−	−	−	+	+	+
PSA in culture medium (ng/ml)	18.07	6.38	8.65	0.87	0.41	7.38	1.16	3.67	20.46

IHC immunohistochemistry, *PSA* prostate-specific antigen

neuroendocrine markers CD56, Chromogranin A and Synaptophysin in three cases. Except from a single, interspersed Chromogranin A-positive cell in one case, these markers stained negative in all cases (supplementary Fig. 2).

Pharmaceutical treatment

Treatment of spheroids with the androgen-receptor antagonist Bicalutamide lead to a significant reduction of cell viability compared to untreated controls (Fig. 4a). This effect was observed after 3 as well as after 5 days and for both cell concentrations. Enzalutamide, a second generation androgen receptor antagonist, was also able to reduce spheroid viability though this effect was not significant in all cases (Fig. 4b; experiment performed using only 10^4 cells due to limited starting material). In contrast, Abiraterone did not show a consistent inhibition of spheroid growth (Fig. 4c). Finally, upon treatment with Docetaxel, spheroids showed a significantly reduced viability after 3 but not after 5 days compared to untreated controls (Fig. 4d). Table 4 gives an overview of the number of cases treated with each compound, their Gleason scores and the response rates. No correlation between the Gleason score and response to any of the used drugs could be observed.

Discussion

This is to date one of the first and the most elaborate study describing the generation and characterization of three-dimensional spheroid cultures from patient-derived tissue specimens of organ-confined PCa.

Caspar et al. (2016) also recently reported on the generation spheroid cultures from RP specimens using a methodology comparable to that of our group on RP tissue from five patients. They could keep their spheroids in culture for up to 84 days and showed that the expression of 11 distinct PCa biomarkers in these spheroids underlies temporal changes as well as interindividual differences. However, no functional studies or further characterization of the spheroid cultures was performed in their study.

The group of Hans Clevers reported on the generation and in-depth molecular characterization of three-dimensional organoid cultures from patients with advanced prostate
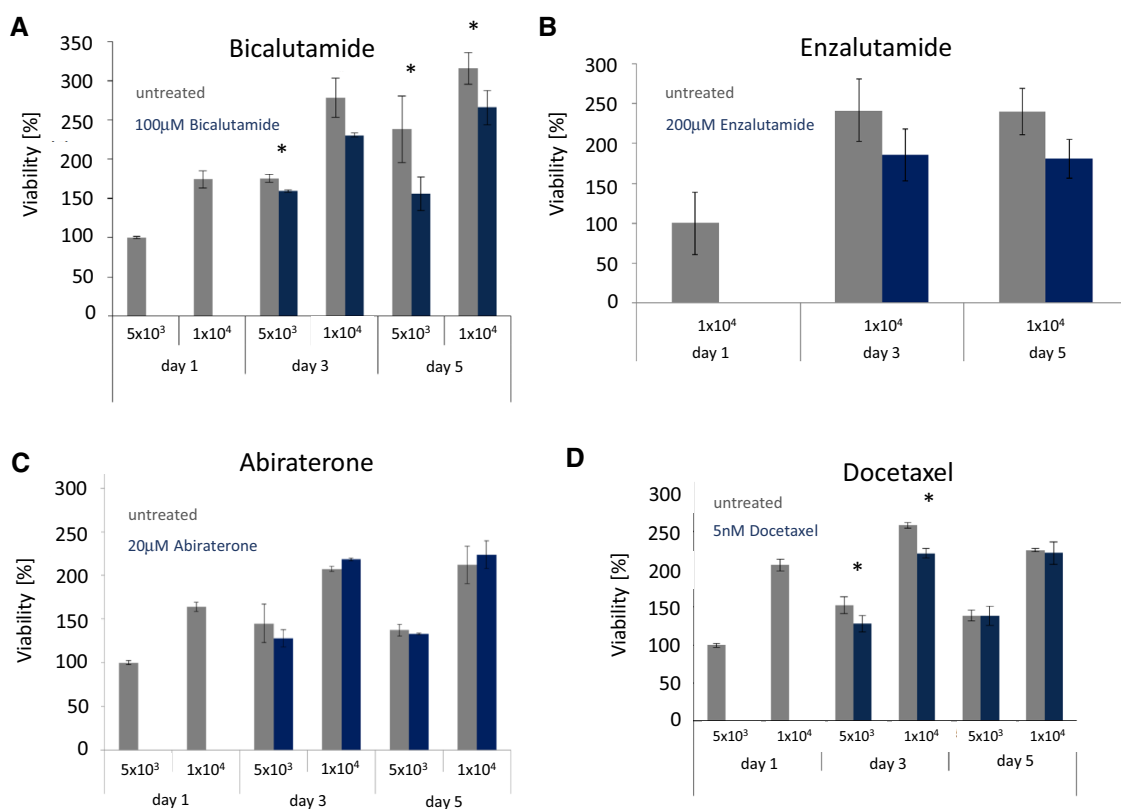
Fig. 4 Pharmaceutical treatment of spheroids. 5×10^3 and (if sufficient cells were available) 1×10^4 cells were seeded in 96-well plates. After spheroids had reformed (at day 1 after seeding), they were subsequently treated with **a** 100 μM Bicalutamide, **b** 200 μM Enzaluta-mide, **c** 20 μM Abiraterone or **d** 5 nM Docetaxel for 5 days. Cell viability was tested using a MTS assay at day 1, 3 and 5 in the untreated and at day 3 and 5 in the treated spheroids. *$p < 0.05$

Table 4 Pharmaceutical treatment of patient-derived spheroids

Drug	Bicalutamide	Enzalutamide	Abiraterone	Docetaxel
No. of cases	8	6	2	2
No. of cases that responded	7 (88%)	5 (83%)	0 (0%)	2 (100%) after 3 days; 0 (0%) after 5 days
Gleason score				
7a	2	1	1	0
7b	2	3	1	2
8	3	1	0	0
9	1	1	0	0

cancer (Gao et al. 2014; Drost et al. 2016). Of interest, they used biopsy specimens (metastases) as well as circulating tumor cells (CTCs) to establish seven long-term organoid cultures, which recapitulated well the molecular diversity of PCa subtypes including *TMPRSS2-ERG* fusion, *SPOP* mutation, *SPINK1* overexpression and *CHD1* loss (Barbieri et al. 2012; Cancer Genome Atlas Research Network 2015). However, they were not able to successfully establish comparable organoid cultures from samples of organ-confined prostate cancer. Of note, in their experienced hands the efficiency for establishing continuously propagated organoid lines from metastatic biopsies was 15–20%, and organoids could be reproducibly maintained for 1–2 months in culture for 70% of soft tissue metastases biopsies and 30% of bone metastases biopsies, respectively. Yet, they reported that many of these tumor cultures were overtaken by tumor-associated spindle cells or normal epithelial cells present in biopsy material. Hence, these organoid lines had no copy number alterations and no mutations in common cancer-associated genes.

Considering this point, our study is limited by the fact that we did not perform genetic/molecular characterization of our spheroids, which could clearly identify or not PCa cells within those. However, the strong AMACR staining in IHC together with CK8 positivity and CK5 negativity in the vast majority of cells strongly suggests the successful isolation and cultivation of cancer cells. This is further substantiated by the fact that we performed frozen-section staining prior to the further processing of the obtained tissue specimens to ensure a sufficiently high proportion of cancer cells. Yet, it would be desirable to provide a definitive proof for the presence of PCa cells, for example by detection of the cancer-specific *TMPRSS2-ERG* fusion gene (Tomlins et al. 2005) or by showing the successful engraftment, growth and spread of the cells after orthotopic implantation in immuno-deficient mice. These experiments are currently under way.

While it could theoretically also be explained by parts of a tumorous intraductal spread, the more probable explanation for the presence of single cells staining positive for the basal marker CK5 and negative for the luminal marker CK8

is a contamination of the initially retrieved tumor tissue samples by non-neoplastic glands. This is also supported by the observation of interspersed non-neoplastic glands between the cancerous cells in the H&E-stained fresh-frozen sections. However, as there is an interaction between malignant and normal prostate epithelial cells in a tumor-bearing gland, we consider it a strength of our model that this interaction can also be represented in contrast to established monoclonal monolayer cultures.

Immunohistochemical staining for the mesenchymal markers vimentin and αSMA showed positive signals in 60–80% of spheroids suggesting the presence of cancer-associated stroma cells, which play an important role in prostate cancer development and progression (Sasaki et al. 2017). Single Ki67-positive cells were observed in one-third of cases. This is consistent with the known low proliferative index of organ-confined prostate cancers (Bubendorf et al. 1996). Importantly, AR, which plays a pivotal role in all stages of prostate cancer (Karantanos et al. 2015), stained positive in 94% of cultivated spheroids. PSA staining was only positive in about one-third of the tested cases, however, elevated PSA-levels in culture medium could be regularly observed irrespective of PSA IHC staining results suggesting an intact secretory function of the cultivated cells. Of note, AR signals were cytoplasmic in the majority of tested patient-derived spheroids with nuclear signals only observed in single cases. The inactive AR is located as monomer in the cytoplasm and dimerizes upon ligand binding, translocates into the nucleus and binds to AR response elements in the DNA. Hence, the most obvious explanation for the cytoplasmic IHC signals in the patient-derived spheroids would be the presence of an inactive AR. However, the detection of elevated PSA levels in the culture media of virtually all cases (PSA is an AR driven gene) as well as the response upon AR-directed therapies (e.g., bicalutamide) strongly argue against an AR inactivity. To gain further insight on this point, we reviewed stainings we performed with the AR antibody used in this study (also those performed in the context other projects) and could observe

that (i) orthotopic LNCaP xenografts show a purely cytoplasmic signal (ii) three-dimensional spheroids generated from LNCaP cells show a mixed nuclear and cytoplasmic signal and that (iii) patient-derived spheroids show some nuclear but mostly a cytoplasmic signal (Supplementary Fig. 3). Based on the considerations discussed above, we suggest that the observation of cytoplasmic AR signals in the patient-derived spheroids is rather a methodological problem than a truly inactive AR (e.g., due to the fixation process).

Response of the spheroids to pharmaceutical treatment was heterogeneous mainly depending on the substance used. While we consistently observed a marked reduction of spheroid viability upon treatment with the androgen receptor antagonists bicalutamide and enzalutamide, abiraterone and docetaxel did not have a profound effect on spheroid viability in the majority of experiments. Yet these results are to be expected considering the mechanisms of action of the used substances as well as the fact that the spheroids were generated from RP tissue specimens, i.e., from comparably low-proliferative organ-confined cancers. The chemotherapeutic docetaxel cannot be expected to have significant effects in spheroids from cancers with a very low proliferative index. The main mechanism of action of abiraterone is to inhibit the enzyme CYP17A1, which plays a role in the adrenal and intratumoral synthesis of testosterone (Sridhar et al. 2014). Yet, in the novel in vitro model established here as well as in any other in vitro model of PCa, adrenal androgen synthesis cannot be displayed. Concerning the second mechanism of action of abiraterone, it is well-known that intratumoral androgen synthesis is mainly an escape mechanism of prostate cancer cells developed upon androgen deprivation therapy leading to castration-resistance. However, as we generated our spheroids from organ-confined, castration-sensitive cancers, it is to be expected that intratumoral androgen synthesis does not yet play a significant role. Furthermore, the mechanism of action of abiraterone is bypassed by the addition of the synthetic androgen R1881 to the culture medium. However, the addition of an androgen to be necessary for spheroid growth in our hands, accordingly it was not possible to perform abiraterone treatment with the spheroids cultured in charcoal-strived medium as is would normally be done.

Our experimental protocol enables the generation, short-term cultivation and characterization of spheroid cultures from RP specimens. Moreover, single functional tests like an analysis of drug sensitivities are possible in the majority of cases. In contrast to established monolayer cultures, the use of patient-derived primary cultures like in our approach ensures an adequate representation of the intertumor-heterogeneity which is a hallmark of PCa. Furthermore, there is no doubt about the advantages of 3D culture systems in

modeling the cellular architecture and nutrient/oxygen gradients of a tumor (Weeber et al. 2017).

However, there are as well some constraints of this technique. First, the amount of available tissue to generate the spheroids is mostly very limited and so is the number of possible downstream experiments—yet this is also true for tissue from metastatic disease or spheroids generated from CTCs (Gao et al. 2014; Drost et al. 2016). Second, there is a quite short period of time during which functional tests can be performed as the viability of the spheroids decreases continually during cultivation. Possible approaches to improve this point could be the co-cultivation with "feeder cells" like fibroblasts (Wang et al. 2015) or further modification of the culture medium. Third, it is not possible to successfully generate vital spheroids from all tissue specimens. Though our success rate to generate spheroids amenable to further experiments is fairly good (109/173 = 63%), there is still much room for improvement.

Conclusions

We established a method to generate three-dimensional spheroid cultures from radical prostatectomy tissue specimens thereby providing an innovative in vitro model to study organ-confined prostate cancer. This constitutes the starting point for further studies, which should aim to improve the applicability of these spheroids for long-term culture and downstream in vitro and in vivo experiments.

Compliance with ethical standards

Conflict of interest The authors declare that they have no conflicts of interest to report.

Informed consent Informed consent for the use of tissue samples from their radical prostatectomy specimens was obtained from all individual participants included in the study.

References

Ahmed HU, El-Shater Bosaily A, Brown LC et al (2017) Diagnostic accuracy of multi-parametric MRI and TRUS biopsy in prostate

cancer (PROMIS): a paired validating confirmatory study. Lancet 389:815–822

Barbieri CE, Baca SC, Lawrence MS et al (2012) Exome sequencing identifies recurrent SPOP, FOXA1 and MED12 mutations in prostate cancer. Nat Genet 44:685–689

Boj SF, Hwang CI, Baker LA et al (2015) Organoid models of human and mouse ductal pancreatic cancer. Cell 160:324–338

Bubendorf L, Sauter G, Moch H et al (1996) Ki67 labelling index: an independent predictor of progression in prostate cancer treated by radical prostatectomy. J Pathol 178:437–441

Cancer Genome Atlas Research Network (2015) The molecular taxonomy of primary prostate cancer. Cell 163:1011–1025

Caspar A, Mostertz J, Leymann M et al (2016) In vitro cultivation of primary prostate cancer cells alters the molecular biomarker pattern. In Vivo 30:573–579

Chen S, Principessa L, Isaacs JT (2012) Human prostate cancer initiating cells isolated directly from localized cancer do not form prostaspheres in primary culture. Prostate 72:1478–1489

Drost J, Karthaus WR, Gao D et al (2016) Organoid culture systems for prostate epithelial and cancer tissue. Nat Protoc 11:347–358

Fizazi K, Tran NP, Fein L et al (2017) Abiraterone plus prednisone in metastatic, castration-sensitive prostate cancer. N Engl J Med 377:352–360

Fraser M, Sabelnykova VY, Yamaguchi TN et al (2017) Genomic hallmarks of localized, non-indolent prostate cancer. Nature 541:359–364

Gao D, Vela I, Sboner A et al (2014) Organoid cultures derived from patients with advanced prostate cancer. Cell 159:176–187

Karantanos T, Evans CP, Tombal B et al (2015) Understanding the mechanisms of androgen deprivation resistance in prostate cancer at the molecular level. Eur Urol 67:470–479

Koppers-Lalic D, Hackenberg M, de Menezes R et al (2016) Non-invasive prostate cancer detection by measuring miRNA variants (isomiRs) in urine extracellular vesicles. Oncotarget 7:22566–22578

Ku SY, Rosario S, Wang Y et al (2017) Rb1 and Trp53 cooperate to suppress prostate cancer lineage plasticity, metastasis, and antiandrogen resistance. Science 355:78–83

Linxweiler M, Linxweiler J, Barth M et al (2012) Sec62 bridges the gap from 3q amplification to molecular cell biology in non-small cell lung cancer. Am J Pathol 180:473–483

Peehl DM (2005) Primary cell cultures as models of prostate cancer development. Endocr Relat Cancer 12:19–47

Sasaki T, Franco OE, Hayward SW (2017) Interaction of prostate carcinoma-associated fibroblasts with human epithelial cell lines in vivo. Differentiation 96:40–48

Shao YH, Demissie K, Shih W et al (2009) Contemporary risk profile of prostate cancer in the United States. J Natl Cancer Inst 101:1280–1283

Shipley WU, Seiferheld W, Lukka HR et al (2017) Radiation with or without antiandrogen therapy in recurrent prostate cancer. N Engl J Med 376:417–428

Siegel RL, Miller KD, Jemal A (2016) Cancer statistics, 2016. CA Cancer J Clin 66:7–30

Sridhar SS, Freedland SJ, Gleace ME et al (2014) Castration-resistant prostate cancer: from new pathophysiology to new treatment. Eur Urol 65:289–299

Tomlins SA, Rhodes DR, Perner S et al (2005) Recurrent fusion of TMPRSS2 and ETS transcription factor genes in prostate cancer. Science 310:644–648

van de Wetering M, Francies HE, Fracis JM et al (2015) Prospective derivation of a living organoid biobank of colorectal cancer patients. Cell 161:933–945

Wang X, Yamamoto Y, Wilson LH et al (2015) Cloning and variation of ground state intestinal stem cells. Nature 522:173–178

Wang S, Gao D, Chen Y (2017) The potential of organoids in urological cancer research. Nat Rev Urol 14:401–414

Weeber F, Ooft SN, Dijkstra KK et al (2017) Tumor organoids as a pre-clinical cancer model for drug discovery. Cell Chem Biol 24:1092–1100

Wong MC, Goggins WB, Wang HH et al (2016) Global incidence and mortality for prostate cancer: analysis of temporal patterns and trends in 36 countries. Eur Urol 70:862–874

Wu X, Gong S, Roy-Burman P et al (2013) Current mouse and cell models in prostate cancer research. Endocr Relat Cancer 20:R155–R170